Prestressing a Space Structure

A. S. K. Kwan* and S. Pellegrino†
Cambridge University,
Cambridge CB2 IPZ, England, United Kingdom

I. Introduction

IT is common practice to preload the joints of a deployable structure after deployment, to remove free play. Recently, global states of prestress have been used to preload groups of joints in a truss structure,[1] to pretension the cables that stiffen the backbone of a deployable mast,[2] and in the shape control of adaptive high-precision trusses.[3,4]

The following problems arise for any specified target state of prestress: 1) where should the prestress actuators, e.g., turnbuckles or piezoelectric actuators, be located; 2) what actuator extensions are required; and 3) what are the best actuator adjustments to improve an existing, incorrect prestress state? These topics are addressed in the following sections. The presentation is focused on pin-jointed trusses but the treatment is valid in general.

Given a statically indeterminate structure with b bars and s independent states of self stress, any state of prestress can be expressed in terms of s coefficients $\boldsymbol{\alpha}$

$$t = S\alpha \tag{1}$$

where S is a self-stress matrix containing s independent states of self stress. The standard compatibility equation for the structure is

$$S^T F S \alpha = -S^T e \tag{2}$$

where $\boldsymbol{e}$ contains b bar extensions.

Section II shows how to find an $\boldsymbol{e}$ that produces $\boldsymbol{t}$ exactly, if there is free choice on the location of s prestress actuators. Section III finds the best approximation to $\boldsymbol{t}$ that can be achieved with a preselected actuators $(0 < a \leq b)$; this treatment is also valid if the target $\boldsymbol{t}$ is not self-equilibrated. Section IV presents a simple optimization scheme for selecting the locations of s actuators that can produce a specified $t = S\alpha$ with minimal extensions. An application to a cable-and-strut structure is described in Sec. V.

II. Actuator Extensions for a Self-Equilibrated t

From Eq. (2) the following set of equations is obtained:

$$S^T e = \beta \tag{3}$$

where $\beta = -S^T F S \alpha$. This is an under-determinate set of equations with $(b-s)$ infinities of solutions. Usually only solutions involving the minimum number of prestress actuators are of practical interest, and the following procedure will produce one of them.

1) Form the augmented matrix $S^T | \beta$.

2) Transform it by row operations into the reduced echelon form $\tilde{S}^T | \tilde{\beta}$ (Ref. 5).

3) Set to zero the $(b-s)$ components of $\boldsymbol{e}$ not corresponding to a pivot in $\tilde{S}^T$.

4) The remaining s extensions are found in $\tilde{\beta}$.

The selection of pivots can be steered toward any preferred actuator locations by putting the preferred bars at the top of $\boldsymbol{e}$; Gaussian eliminations with partial pivoting look for pivots in these columns first.

Received May 29, 1992; revision received April 6, 1993; accepted for publication April 6, 1993.

*Research Associate, Engineering Department, Trumpington Street.
†Lecturer, Engineering Department, Trumpington Street.

III. Best Approximation to t with a Preselected Actuators

In this section we compute t_{LS}, the least squares (LS) approximation to a specified $\boldsymbol{t}$, and the corresponding extensions of the available actuators. The vector $\boldsymbol{e}$ contains only a nonzero components, hence Eq. (2) becomes

$$-\bar{S}^T \bar{e} = S^T F S \alpha \tag{4}$$

where $\bar{e}$ contains the a actuator extensions, and $\bar{S}$ is the corresponding reduced self-stress matrix. Premultiplying both sides of Eq. (4) by $S(S^T F S)^{-1}$ yields

$$-S(S^T F S)^{-1} \bar{S}^T \bar{e} = S\alpha \tag{5}$$

which relates actuator extensions $\bar{e}$ and prestress $S\alpha$. In general, Eq. (5) may admit one or more solutions, if the specified $\boldsymbol{t}$ can be achieved with the available actuators, or no solution if $\boldsymbol{t}$ cannot be achieved with these actuators. More general prestress states can be considered by replacing the right-hand side of Eq. (5) with $\boldsymbol{t}$. Thus, having introduced

$$A = -S(S^T F S)^{-1} \bar{S}^T \tag{6}$$

the following system of b equations in a unknowns is obtained

$$A\bar{e} = t \tag{7}$$

The LS solution of Eq. (7), coinciding with the exact solution if there is one, can be obtained from the singular value decomposition of $A = U\Sigma V^T$. The LS approximation to e_{LS} (Ref. 6) is

$$\bar{e}_{LS} = \sum_{i=1}^{r} \frac{u_i^T t}{\sigma_i} v_i \tag{8}$$

from which $t_{LS} = A\bar{e}_{LS}$. Here, $r = \text{rank}(A)$ and the singular values σ_i are greater than a small tolerance, and u_i and v_i are the singular vectors of A. This algorithm can cope with rank-deficient LS problems if $r < a$, thus generalizing the algorithm in Refs. 3 and 4.

IV. Optimal Actuator Location for a Self-Equilibrated t

Sometimes it is useful to have an automatic selection procedure based on an optimality criterion. Because small extensions are generally desirable, for more compact actuators and less geometrical distortion, a commonly used criterion is to minimize overall actuator extension

$$\sum_{i=1}^{b} |e_i| \tag{9}$$

Of course, no more than s actuators should be considered at any one time, but this condition is naturally satisfied by the method proposed here.

The optimization of Eq. (9) subject to the constraint of Eq. (3) can be cast in the form of a standard linear program (LP) by introducing two sets of nonnegative variables e^+ and e^-, such that $e_i = e_i^+ - e_i^-$. Thus $|e_i| = e_i^+ + e_i^-$, and the problem is to minimize

$$\sum_{i=1}^{b} (e_i^+ + e_i^-)$$

subject to

$$[|S^T| - S^T] \begin{bmatrix} e^+ \\ e^- \end{bmatrix} = \beta \text{ and } e_i^+ \geq 0,\ e_i^- \geq 0$$

Next, it will be shown that this problem has a solution. First, a basic feasible solution, satisfying all of the constraints and with only s nonzero entries, is constructed after computing $\boldsymbol{e}$, see Sec. II. Of the s nonzero entries of $\boldsymbol{e}$, positive numbers go into the corresponding entries of e^+ and negative numbers into e^-, after reversing their signs. The objective function (9) is nonnegative, and hence the LP cannot be unbounded. Therefore, starting from the basic feasible solution obtained earlier, an optimal solution can be obtained by the simplex method.[7]

V. Application to a Deployable Structure

Figure 1 shows, in plan view, a deployable structure that is part of the back-up structure for a deployable mesh antenna. It consists of 36 cables, 1–12 in plane and 13–36 out of plane, and 24 bars (drawn thicker). These elements lie on the edges of six octahedral modules, each containing four bars and eight cables, and many in-plane cables are shared among two units. In the real structure joints A–F are connected to deployable masts and can be drawn toward O to fold the structure. All of the joints will be modeled as frictionless spherical hinges, and only the deployed configuration will be analyzed, hence all of the cables are taut.

Figure 2 illustrates the structural concept, two equal and opposite forces applied to opposite corners of an octahedral module induce tensile forces in the eight edge members connected to the loaded corners and compressive forces in the remaining four members. Any number of modules can be connected and prestressed in this way, thus all elements in the three modules shown in the figure carry unit forces for the loading shown. This simple structure can be made with 12 bars and 24 cables. The structure shown in Fig. 1 is based on the three-module string AF, the two-module string BE, and the single module CD; hence, the state of prestress obtained by superposition of three stress states based on Fig. 2 is certainly statically admissible. The resulting state of prestress is nearly uniform: the inner in-plane cables 3, 5, 7, 8, 10, and 11 carry a pretension of 2 N and all other members have a prestress of − 1 N. This is the prestress state that we shall aim for.

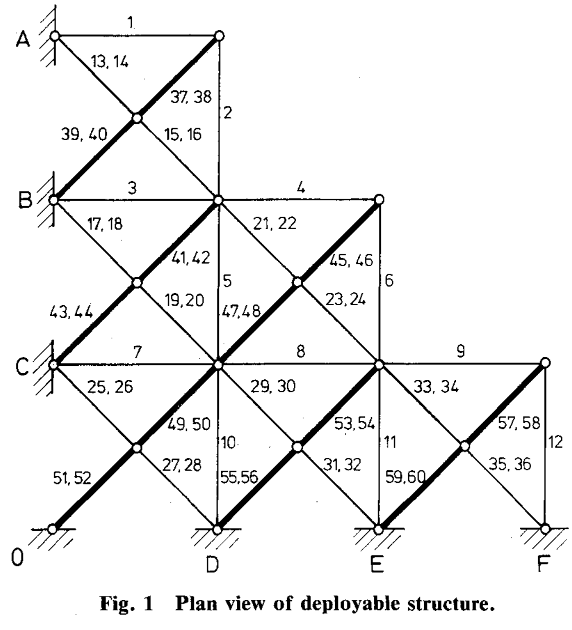

Fig. 1 Plan view of deployable structure.

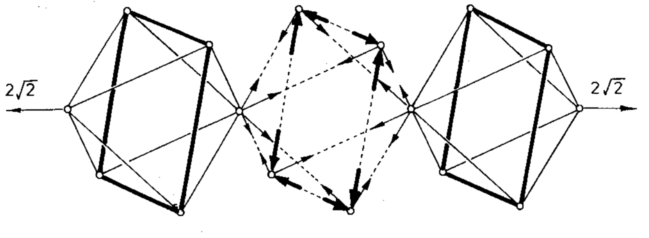

Fig. 2 Uniform prestress state induced by equal and opposite end forces.

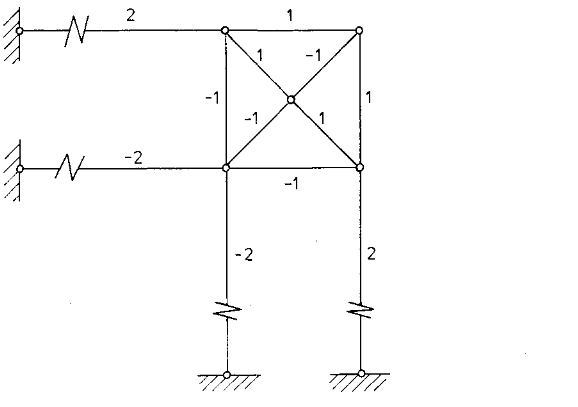

Fig. 3 General state of self stress, plan view.

Actually, $s = 6$ for this structure, and the simplest way of generating six independent states of self-stress is from the self-stress cell shown in Fig. 3, involving a single octahedral module and the in-plane cables connecting it to the supports. The α corresponding to our target prestress is $\alpha = [1 \ \ 1 \ \ 1 \ \ 1 \ \ 1 \ \ 1]^T$.

Different ways of setting up the required state of prestress have been compared for a structure with 500-mm-long elements, $(AE)_{\text{cables}} = 9.8\ 10^4$ N and $(AE)_{\text{bars}} = 3.5\ 10^6$ N. All of the extensions are in millimeters.

1) Actuators in members 1, 3, 4, 7, 8, and 9. For this particular choice, Eq. (3) has the solution

$$[e_1 \ e_3 \ e_4 \ e_7 \ e_8 \ e_9] = 10^{-3}[-155.0 \ \ -93.1 \ \ 123.8 \ \ -41.5 \ \ 31.2 \ \ -41.5]$$

with

$$\sum |e_i| = 0.486$$

2) Optimal set. The procedure of Sec. IV has produced

$$[e_1 \ e_3 \ e_5 \ e_7 \ e_{10} \ e_{11}] = 10^{-3}[-10.4 \ \ -0.1 \ \ -32.5 \ \ -10.0 \ \ -72.7 \ \ -51.7]$$

with

$$\sum |e_i| = 0.176$$

3) 1500 randomly chosen sets of six actuators such that rank($\bar{S}$) = 6 have produced a solution, involving members 7, 8, 10, 27, 30, and 46, with $\Sigma |e_i| = 0.217$.

VI. Final Remark

In practice, the actuator extensions computed with the provided algorithms may still produce an error Δt, due to inaccurate modeling of joints, mechanical tolerances, etc. This Δt may not be self-equilibrated, but the algorithm of Sec. III will produce the best corrections Δe.

Acknowledgments

Support from the Science and Engineering Research Council is gratefully acknowledged. S. Pellegrino gratefully acknowledges the award of an ESA Fellowship. We thank C. R. Calladine and K. Glover for helpful discussions, B. K. Wada for sending us reprints of his work, and a referee for helpful comments on an earlier version of this Note.

References

[1]Panin, F., Eiden, M., Sierra, M., and Rivacoba, J., "A Sequentially Deployable Structure for Space Applications," *Proceedings of Third European Mechanisms and Tribology Symposium* (Madrid, Spain), ESA, Noordwijk, The Netherlands, 1987, pp. 73–82.

[2]Kwan, A. S. K., and Pellegrino, S., "The Pantographic Deployable Mast: Design, Structural Performance and Deployment Tests," *Rapidly Assembled Structures,* edited by P. S. Bulson, Computational Mechanics, Southampton, England, UK, 1991, pp. 213–224.

[3]Baycan, C. M., Utku, S., Das, S. K., and Wada, B. K., "Optimal Actuator Placement in Adaptive Precision Trusses," *Proceedings of the AIAA/ASME/ASCE/AHS 33rd Structures, Structural Dynamics, and Materials Conference,* AIAA, Washington, DC, 1992, pp. 418–423.

[4]Jalihal, P., Utku, S., and Wada, B. K., "Optimal Location of Redundants for Prestressing Adaptive Trusses with Buckling Considerations," *Proceedings of AIAA/ASME/ASCE/AHS 33rd Structures, Structural Dynamics, and Materials Conference,* AIAA, Washington, DC, 1992, pp. 412–417.

[5]Strang, G., *Linear Algebra and its Applications,* 2nd ed., Academic Press, New York, 1980, Chap. 2.

[6]Golub, G. H., and Van Loan, C. F., *Matrix Computations,* North Oxford Academic, Oxford, England, UK, 1983, Chap. 6.

[7]Luenberger, D. G., *Linear and Nonlinear Programming,* Addison-Wesley, Reading, MA, 1984, Chap. 3.

Transverse Shear Deformation in Exact Buckling and Vibration of Composite Plate Assemblies

Melvin S. Anderson*
Old Dominion University Research Foundation, Norfolk, Virginia 23508
and
David Kennedy†
University of Wales, College of Cardiff, Cardiff CF2 1YF, Wales, United Kingdom

Introduction

THE program VICONOPT[1] performs buckling and vibration analysis and optimum design of any prismatic assembly of composite plates. The analysis assumes that the response in the longitudinal direction is a summation of sinusoidal responses and that individual plates have stiffness properties resulting from balanced symmetric laminates. It uses stiffness matrices derived analytically from the exact solution of the uncoupled in-plane and out-of-plane fourth-order differential equations of classical plate theory. The introduction of transverse shear deformation makes the out-of-plane equation sixth order, necessitating a numerical solution. In this Note the numerical solution is developed in a general way to include the coupled case that has order $N = 10$ when transverse shear is included and order $N = 8$ otherwise, so allowing the exact treatment of any laminate with an arbitrarily located reference surface.

The usual numerical approach involves writing the coupled plate equilibrium equations in terms of displacements and determining the characteristic roots from the associated determinant. This approach leads to complicated expressions that are impractical to implement for the most general cases. Alternatively, Cohen[2] wrote the differential equations as a first-order system with the displacements and the associated forces as unknowns. The resulting matrix is much simpler and can be arranged so that the characteristic root appears only on the diagonal, so that a standard linear eigenvalue solver can be used. The eigenvectors give the relationships between all of the forces and displacements.

Because exact stiffness expressions are used, plates need not be subdivided to obtain accuracy. Nodes are required only at junctions of two or more plates. At such junctions, continuity of rotation requires that the shear angle in the plane of the edge forming a junction must be zero unless all plates are coplanar. By using the shear angle as the additional unknown over classical plate theory, as in Cohen,[2] the continuity condition is satisfied by deleting the rows and columns of the plate stiffness matrix corresponding to the shear angle. This results in a stiffness matrix with the same unknowns as classical plate theory, and the assembly of the global stiffness matrix from individual plate stiffnesses is unchanged.

This Note summarizes the development of the theory for which Ref. 3 gives a complete description, including all necessary equations for its direct implementation and typical results obtained from its application.

Governing Plate Equations

It is assumed that the plate has fully populated $\underline{A}$, $\underline{B}$, and $\underline{D}$ stiffness matrices with its reference surface arbitrarily located in the x-y plane as shown in Fig. 1. First-order shear deformation theory, where the in-plane displacements u and v vary linearly with z, is assumed. The plate is loaded by uniform in-plane stress resultants (see Fig. 1a) acting at a distance z_c from the reference surface in the centroidal plane of the cross section treated as a wide beam. Figure 1b shows the additional forces and moments that occur during buckling or the amplitudes of such forces during vibration at a frequency ω. Deflection in all three directions is resisted by Winkler elastic foun-

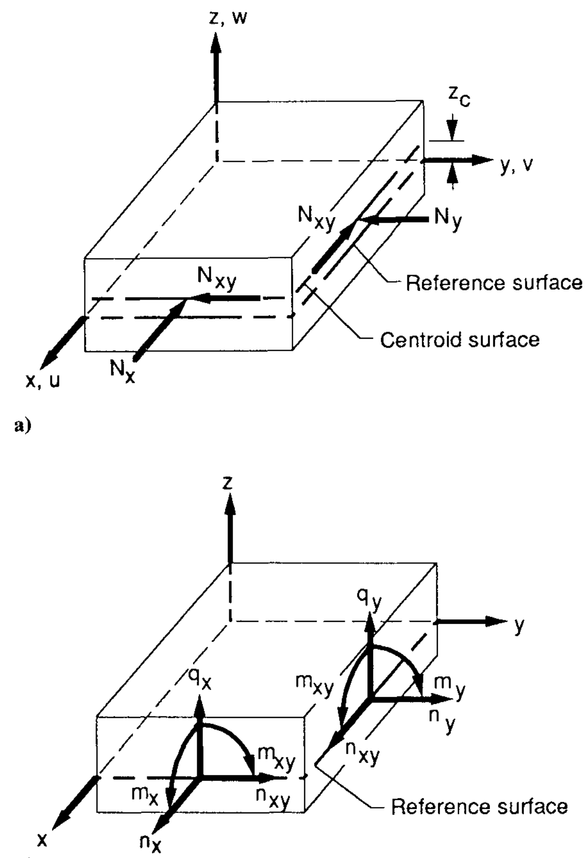

Fig. 1 Positive directions of forces and moments per unit width acting on a plate element: a) prebuckling in-plane loads (N_x, N_y, N_{xy}) and b) buckling in-plane forces (n_x, n_y, n_{xy}), moments (m_x, m_y, m_{xy}), and transverse shearing forces (q_x, q_y).

Received Feb. 12, 1992; presented as Paper 92-2287 at the AIAA/ASME/ASCE/AHS/ASC 33rd Structures, Structural Dynamics, and Materials Conference, Dallas, TX, April 13–15, 1992; revision received April 13, 1993; accepted for publication April 27, 1993.

*Research Professor, NASA Langley Research Center, Hampton, VA 23681. Associate Fellow AIAA.

†Lecturer/Senior Research Associate, School of Engineering, P.O. Box 925.